Reciprocity Basis for EEG Source Imaging

Leonid Zhukov
SCI Institute
University of Utah
zhukov@cs.utah.edu

David Weinstein
SCI Institute
University of Utah
dmw@cs.utah.edu

Chris Johnson
SCI Institute
University of Utah
crj@cs.utah.edu

1 Introduction

The distribution of an electromagnetic field in the head is described by the linear Poisson equation:

$$\nabla \cdot (\sigma \nabla \phi) = \nabla \cdot \mathbf{J}^{\mathbf{s}}, \text{ in } \Omega \tag{1}$$

with no-flux Neumann boundary conditions on the scalp:

$$\sigma(\nabla \phi) \cdot \mathbf{n} = 0, \text{ on } \Gamma_{\Omega} \tag{2}$$

From the linearity of (1), it follows that the mapping from electric sources within the cranium to scalp recordings on the outside of the scalp can be represented by a linear operator $\mathbf{L}$. Given a particular configuration of sources, $\mathbf{s}$, the resultant recordings, $\boldsymbol{\phi}_r$, and the noise in the system, $\mathbf{n}$, we represent this relation as

$$\boldsymbol{\phi}_r = \mathbf{L}\mathbf{s} + \mathbf{n} \tag{3}$$

$\mathbf{L}$ is the so-called *lead-field matrix* and contains information about the geometry and conductivity of the model.

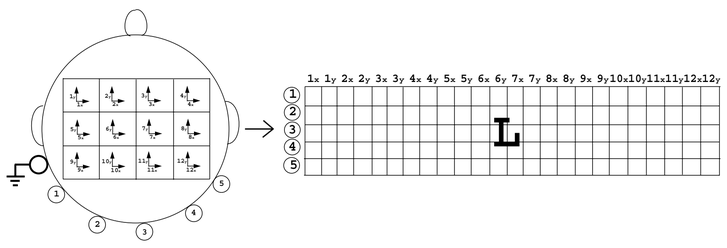

The traditional method of constructing the $\mathbf{L}$ matrix is to place three orthogonal sources in each cell of a volume domain, and for each dipole source, compute the voltages at the electrodes. For a volume mesh consisting of N tetrahedral elements, this requires computing $(N \times 3)$ forward solutions.

2 Finite Element Model

The main idea behind the FEM is to reduce a continuous problem with infinitely many unknown field values to a finite number of unknowns by discretizing the solution region into elements. The value at any point in the field can then be approximated by interpolation functions within the elements. These interpolation functions are specified in terms of the field values at the corners of the elements, points known as nodes. We note that for linearly interpolation potentials, the electric field is constant within an element.

Given a geometric model, the FEM proceeds by assembling the matrix equations to build the stiffness matrix $\mathbf{A}$. This can be done using, for example, a Rayleigh-Ritz or Galerkin method. Boundary conditions are then imposed and source currents are applied. These boundary and source conditions are incorporated within the right hand side of the system (vector $\mathbf{b}$). Application of the FEM reduces Poisson's equation to the linear system:

$$\mathbf{A}_{ij}\boldsymbol{\phi}_j = \mathbf{b}_i \tag{4}$$

where ϕ are the unknown potentials at the nodes of the volume.

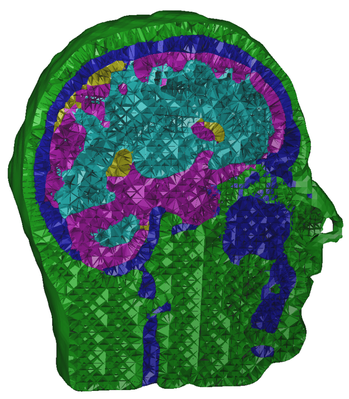

The realistic head geometry was obtained from MRI data, where the volume was segmented and each tissue material was labeled in the underlying voxels. The segmented head volume was then tetrahedralized via a mesh generator that preserved the classification when mapping from voxels to elements. For each tissue classification, we assigned a conductivity tensor from the literature. A cut-through of the classified mesh is shown in the figure above.

When we use a realistic FEM model (3mm resolution), and the above forward numerical construction, we may require upwards of a minute of CPU time on modern architectures (*e.g.*, an SGI MIPS R10000 processor) to solve a forward simulation. Because of this computational expense, it seems feasible to build a lead-field for only a very sparse grid of sources. Even a 16^3 grid (12mm resolution), for example, with three orthogonal dipole components per cell, would require over a day of continuous computation to build $\mathbf{L}$.

3 Reciprocity Principle

The reciprocity principle states that given a dipole (an equivalent source), $\mathbf{p}$, and a need to know the resulting potential difference between two points A and B, it is sufficient to know the electric field $\mathbf{E}$ at the dipole location resulting from a current, I, placed between points A and B:

$$\frac{(\mathbf{E} \cdot \mathbf{p})}{-I} = \phi_{\mathbf{A}} - \phi_{\mathbf{B}} \tag{5}$$

So, rather than iteratively placing a source in every element and computing a forward solution at the electrodes, we can "invert" this process: we place a source and sink at pairs of electrodes, and for each pair compute the resulting electric field in all of the elements. We can then use the reciprocity principle to reconstruct the potential differences at the electrodes for a source placed in any element.

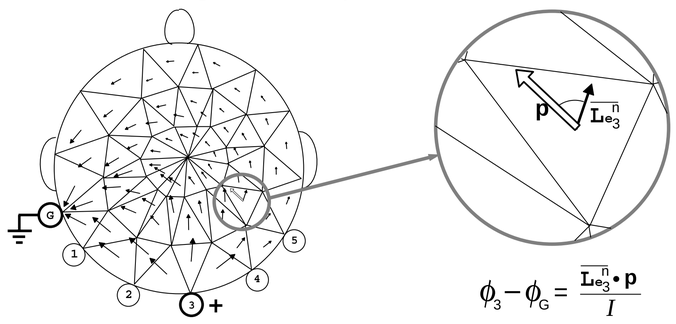

In constructing the $\mathbf{L}$ matrix, we would like to achieve the maximal possible resolution of sources for our model: one dipole per tetrahedral element. We would also like to take advantage of the fact that when using the FEM, we compute the potentials not only on the surfaces (as in the boundary element method), but through the entire volume. We can achieve both goals using the *principle of reciprocity*.

4 Lead-field Basis

The algorithm for the L matrix construction:

- Choose one electrode as ground (*i.e.*,force its potential to be zero).
- Choose one of the other electrodes, place a current source, I, perpendicular to the surface at that electrode and a current sink at the ground electrode.
- Compute the forward solution, resulting in a potential field, ϕ, defined at each node in the domain.
- Take the gradient of this potential field, yielding the electric field, $\mathbf{E}$, at each element in the head.
- Compute rows of the lead field $\mathbf{L_e}$ by evaluating $\mathbf{E}/-I$ in every element.
- Repeat this process for each of the M source electrodes

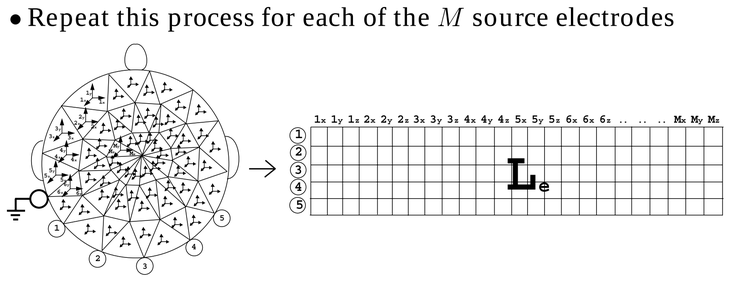

Constructed $\mathbf{L_e}$ matrix will then satisfy:

$$\begin{bmatrix} L_1^{1,x} & L_1^{1,y} & L_1^{1,z} & \dots & L_1^{N,x} & L_1^{N,y} & L_1^{N,z} \\ L_2^{1,x} & L_2^{1,y} & L_2^{1,z} & \dots & L_2^{N,x} & L_2^{N,y} & L_2^{N,z} \\ \dots & \dots & \dots & \dots & \dots & \dots & \dots \\ L_M^{1,x} & L_M^{1,y} & L_M^{1,z} & \dots & L_M^{N,x} & L_M^{N,y} & L_M^{N,z} \end{bmatrix} \cdot \begin{bmatrix} s_{1,x} \\ s_{1,y} \\ s_{1,z} \\ .. \\ s_{N,x} \\ s_{N,y} \\ s_{N,z} \end{bmatrix} = \begin{bmatrix} \phi_1 \\ \phi_2 \\ .. \\ \phi_M \end{bmatrix} \tag{6}$$

5 Applications

One of the simplest applications of the $\mathbf{L_e}$ operator is to construct a single dipole *cost-function field*. The cost-function field is constructed as follows:

- position a dipole in an element;
- find the optimal magnitude and orientation for the dipole in that element using linear least squares optimization (all locations within the same element are equivalent);
- compute the two-norm misfit between the forward solution $\hat{\phi}$ due to that dipole, and the "measured" data, ϕ.

Repeating the above steps for all the elements in the model, we construct the cost-function field:

$$C_n = ||\phi - \hat{\phi}|| = ||\phi - \bar{p}_x \mathbf{L_e^{n,z}} - \bar{p}_y \mathbf{L_e^{n,y}} - \bar{p}_z \mathbf{L_e^{n,z}}|| \tag{7}$$

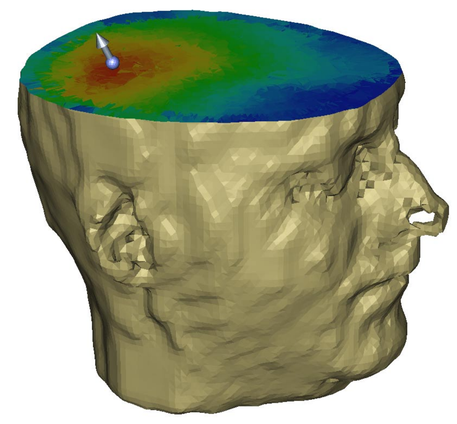

The misfit between the "measured" data (due to the depicted dipole source) and the forward solution due to the optimal source for each element has been color mapped to an axial cutting plane. Blue values correspond to a large misfit, whereas red values correspond to a very small misfit.

Clearly, the minimum of this field corresponds to the optimal dipole position for a single dipole model.

6 BioPSE Simulations

To verify the accuracy and usability of the basis, we constructed a realistic finite element head model from a volume MRI scan. The model contains

- $320,000$ elements
- $60,000$ nodes
- 6 different conductivity regions

Using our method, we first computed the reciprocity $\mathbf{L}$ basis which required 9 minutes of CPU time. We then used the basis to construct and visualize a single dipole cost-function field, i.e. misfit between the measured data and the sequence of forward solutions. The minimum of this field corresponds to the optimal dipole position for a single dipole model.

All the computations and visualization for this paper were performed within the BioPSE. BioPSE is a scientific programming environment that allows the interactive construction, debugging, and steering of large-scale scientific computations.

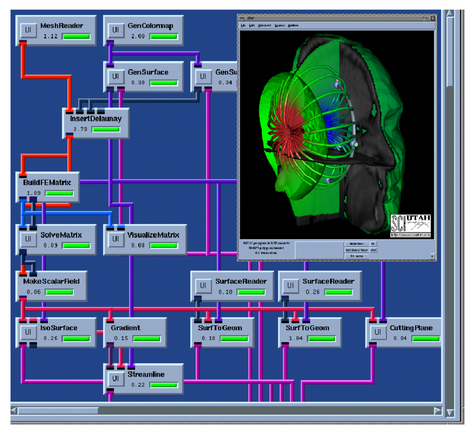

Acknowledgments

This work was supported in part by the National Science Foundation, the Department of Energy, the National Institutes of Health, and the Utah State Centers of Excellence Program.